

## Isotropic second-order nonlinear optical susceptibilities

Peer Fischer,<sup>1,\*</sup> A. D. Buckingham,<sup>2,†</sup> and A. C. Albrecht<sup>1,‡</sup><sup>1</sup>*Department of Chemistry, Cornell University, Ithaca, New York 14853-1301*<sup>2</sup>*Department of Chemistry, University of Cambridge, Lensfield Road, Cambridge CB2 1EW, United Kingdom*

(Received 4 June 2001; published 16 October 2001)

The second-order nonlinear optical susceptibility, in the electric dipole approximation, is only nonvanishing for materials that are noncentrosymmetric. Should the medium be isotropic, then only a chiral system, such as an optically active liquid, satisfies this symmetry requirement. We derive the quantum-mechanical form of the isotropic component of the sum- and difference-frequency susceptibility and discuss its unusual spectral properties. We show that any coherent second-order nonlinear optical process in a system of randomly oriented molecules requires the medium to be chiral, and the incident frequencies to be different and nonzero. Furthermore, a minimum of two nondegenerate excited molecular states are needed for the isotropic part of the susceptibility to be nonvanishing. The rotationally invariant susceptibility is zero in the static field limit and shows exceptionally sensitive resonance and dephasing effects that are particular to chiral centers.

DOI: 10.1103/PhysRevA.64.053816

PACS number(s): 42.65.An, 42.65.Ky, 42.62.Fi

### I. INTRODUCTION

Second-order nonlinear optical materials derived from organic or polymeric synthesis find application in optical signal processing, e.g., frequency conversion, parametric amplification, and electrooptic amplitude or phase modulation [1]. For a material to exhibit a coherent second-order nonlinear optical response it needs to be noncentrosymmetric on a macroscopic scale. However, most liquids, amorphous materials, sol-gels, and polymers are centrosymmetric (and isotropic). Even crystals of dipolar molecules often show only a weak, or no, quadratic nonlinearity, as dipoles can favor an antiparallel alignment. To overcome macroscopic centrosymmetry, one has to induce anisotropy either by specifically tailoring molecules that crystallize in a noncentrosymmetric space group [2], or by preferentially aligning dipolar chromophores in a static electric field (poling) [3]. Poled materials, however, tend to show unwanted birefringence and the induced polar order often diminishes with time. An altogether different approach to breaking centrosymmetry, and thus allowing for second-order nonlinear optics to occur even in an isotropic medium, is to use chiral molecules [4].

In any isotropic medium, the macroscopic quadratic nonlinearity, the second-order non-linear susceptibility, is a pseudoscalar ( $\chi^{(2)}$ ) and is proportional to the rotationally invariant component of the molecular first hyperpolarizability tensor  $\bar{\beta}$ . In a medium of randomly oriented molecules, both  $\chi^{(2)}$  and  $\bar{\beta}$  are only sensitive to the chiral centers and exist only for nondegenerate sum- and difference-frequency generation (SFG and DFG) [4]. Isotropic chiral systems with an appreciable nonlinearity would not only be of interest as quadratic nonlinear media, but since chiral centers are ubiquitous in both proteins and nucleic acids, such a method to study their spectroscopy and dynamics, in the absence of any background, would be of interest in biophysics.

A recent study finds that the isotropic part of the SFG hyperpolarizability is, in the absence of resonance, three orders of magnitude smaller than any other  $\beta_{ijk}$  tensor component [5–7], and a nonresonant bulk SFG signal is therefore difficult to detect. Quite recently, a vibrationally resonant sum-frequency signal has been observed in resolved solutions of limonene, and its infrared (IR) resonant  $\bar{\beta}$  has been found to be about three orders of magnitude smaller compared to its other IR-resonant components  $\beta_{ijk}$  [8]. In this paper, we search for reasons behind the evident fragility of the SFG (and DFG) signal from an isotropic chiral medium and suggest ways for its optimization [9].

### II. THE ISOTROPIC SECOND-ORDER SUSCEPTIBILITY $\chi^{(2)}$

The optical nonlinearities at second order may give rise to three-wave mixing, where two electromagnetic fields interact in a nonlinear medium to induce a (quadratic) polarization vector  $P_\alpha^{(2)}$  at the sum and difference frequencies [10,11]. For two monochromatic fields  $E_\beta(\omega_1)$  and  $E_\gamma(\omega_2)$ , the polarization at the sum-frequency  $\omega_S$  and difference-frequency  $\omega_D$  is in the electric dipole approximation given by

$$P_\alpha^{(2)}(\omega_S = \omega_1 + \omega_2) = \epsilon_0 \chi_{\alpha\beta\gamma}^{(2)}(\omega_S = \omega_1 + \omega_2) E_\beta(\omega_1) E_\gamma(\omega_2),$$

$$P_\alpha^{(2)}(\omega_D = -\omega_1 + \omega_2) = \epsilon_0 \chi_{\alpha\beta\gamma}^{(2)}(\omega_D = -\omega_1 + \omega_2) \times E_\beta^*(\omega_1) E_\gamma(\omega_2), \quad (1)$$

where  $\chi_{\alpha\beta\gamma}^{(2)}$  is a second-order nonlinear susceptibility tensor and the star denotes complex conjugation.

The intensity at the sum or difference frequency is proportional to the square modulus of the polarization,  $|P_\alpha^{(2)}|^2$ , and the coherent buildup of radiation at the sum or difference frequency requires, apart from a nonvanishing susceptibility, that the polarization and the field generated from it be phase matched. However, the phase-matching criterion is, in general, not met for SFG or DFG under conditions of normal dispersion [5]. In what follows, we will assume that either

\*Electronic address: pf43@cornell.edu

†Electronic address: adb1000@cam.ac.uk

‡Electronic address: aca7@cornell.edu

the path length of the interacting waves is sufficiently short in the bulk, but remains distinguishable from any surface contributions, or (less likely) that the medium exhibits anomalous dispersion, so as to allow for phase-matched SFG or DFG from the bulk [12].

In an isotropic medium, a bulk physical property tensor, such as the susceptibility  $\chi^{(2)}$ , is necessarily independent of the orientation of the frame of reference in which it is evaluated. It follows that only those tensor components are non-vanishing that are rotationally invariant. From a total of 27 components for the third-rank tensor  $\chi_{\alpha\beta\gamma}^{(2)}$ , only the following six components

$$\chi_{xyz}^{(2)} = -\chi_{xzy}^{(2)} = \chi_{yzx}^{(2)} = -\chi_{yxz}^{(2)} = \chi_{zxy}^{(2)} = -\chi_{zyx}^{(2)} \quad (2)$$

are nonzero in an isotropic medium, in any Cartesian basis  $x, y, z$ . It is convenient to express the susceptibility components in Eqs. (1) and (2) in the coordinates of the laboratory frame that is also the frame of the incident radiation and that we shall denote by  $I, J, K$ . These are, in turn, related to components of the microscopic first hyperpolarizability  $\beta$ , which are best written in terms of a molecule-fixed frame,  $i, j, k$ . Thus, we have

$$\chi_{IJK}^{(2)} = \frac{N\beta_{ijk}}{\epsilon_0} \langle a_{iI} a_{jJ} a_{kK} \rangle, \quad (3)$$

where  $a_{iI}, a_{jJ}$ , and  $a_{kK}$  are direction cosines linking the two frames of reference, and  $\langle \dots \rangle$  denotes a statistical average over the orientation of the molecular species whose number density is  $N$ .<sup>1</sup> As is appropriate for any isotropic medium such as a gas or a liquid, an unweighted orientational average is taken. It follows that the isotropic component  $\chi^{(2)}$  of the second-order susceptibility  $\chi^{(2)}$  is directly proportional to the completely antisymmetric component of the first hyperpolarizability tensor, i.e.,

$$\begin{aligned} \chi^{(2)} &= \frac{N}{\epsilon_0} \frac{1}{6} (\beta_{xyz} - \beta_{xzy} + \beta_{yzx} - \beta_{yxz} + \beta_{zxy} - \beta_{zyx}) \\ &= \frac{N}{\epsilon_0} \frac{1}{6} \epsilon_{\alpha\beta\gamma} \beta_{\alpha\beta\gamma} \equiv \frac{N}{\epsilon_0} \bar{\beta}, \end{aligned} \quad (4)$$

where  $\epsilon_{\alpha\beta\gamma}$  is the Levi-Civita tensor. It is seen that the isotropic component of the electric dipolar first hyperpolarizability changes sign for a molecule that possesses a mirror plane of symmetry, hence, it follows that the pseudoscalar  $\bar{\beta}$  is only symmetry allowed in a chiral molecule (a molecule that is distinct from its mirror image). Since  $\bar{\beta}$  is of opposite sign for optical isomers,  $\chi^{(2)}$  is zero in a racemic mixture. Thus, the concentration  $N$  of the optically active enantiomer and  $\bar{\beta}$  determine the macroscopic second-order susceptibility in any isotropic system.

<sup>1</sup>We note that in time-dependent perturbation theory the link between the macroscopic susceptibility and the molecular hyperpolarizability at  $n$ th order contains a divisor of  $n!$  on the rhs of Eq. (3). This factor is absent in the time-ordered density matrix approach used here.

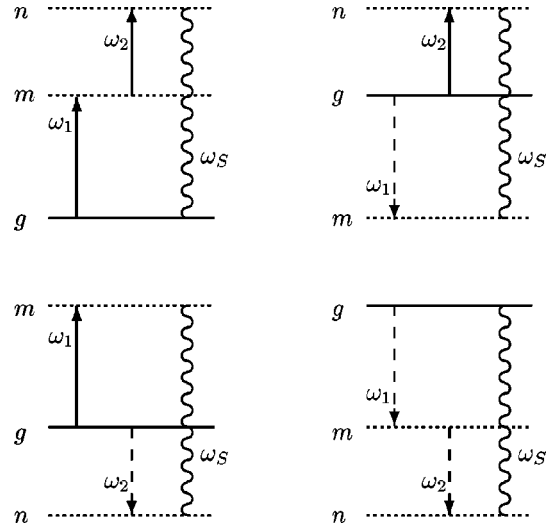


FIG. 1. The four basic WMEL diagrams (equivalent to double-sided Feynman diagrams) are depicted for sum-frequency generation ( $\omega_S = \omega_1 + \omega_2$ ). Solid arrows indicate *ket* evolution, dashed arrows show the *bra* evolution. The ground-state  $g$  is represented by the solid-horizontal line, while the dashed-horizontal lines represent virtual states  $m$  and  $n$  of the basis set. (When resonant, these would become solid lines in a WMEL diagram.) The acting Fourier components of the two incident fields are given by their (signed) frequencies. All eight diagrams are obtained by including the permutations of the ordering of the incident fields, i.e.,  $\omega_1 \leftrightarrow \omega_2$ .

### III. THE ISOTROPIC COMPONENT OF THE FIRST HYPERPOLARIZABILITY

Time-dependent perturbation theory may be used to obtain a sum-over-states expression for the frequency-dependent first hyperpolarizability. In a density-matrix formalism, there are eight Liouville paths to be considered at second order. Each path defines a particular time ordering of the actions of the two incident fields that act either on the bra or ket side of the molecule's basis set [11,13]. Figures 1 and 2 show the four basic Liouville paths as wave-mixing energy level (WMEL) diagrams for SFG and DFG, respectively. After permuting the time ordering of the incident fields  $\omega_1$  and  $\omega_2$  for SFG ( $-\omega_1$  and  $\omega_2$  for DFG) all eight diagrams at second order are obtained for each process. The isotropic component of the full analytical sum-over-states expression for the hyperpolarizability  $\bar{\beta}$  at the sum-frequency  $\omega_S$  and the difference-frequency  $\omega_D$  is expressible in the simple form

$$\bar{\beta}(\omega_D = \pm \omega_1 + \omega_2) \equiv \sum_{m,n} \overline{\mu^{(3)}}(m,n) \mathcal{F}(\omega_D) (\omega_S) (m,n), \quad (5)$$

where

$$\overline{\mu^{(3)}}(m,n) \equiv \frac{1}{6} \boldsymbol{\mu}_{gm} \cdot (\boldsymbol{\mu}_{mn} \times \boldsymbol{\mu}_{ng}) = \frac{1}{6} \epsilon_{\alpha\beta\gamma} \mu_{gm\alpha} \mu_{mn\beta} \mu_{ng\gamma} \quad (6)$$

and

$$\begin{aligned}
\mathcal{F}_{(\omega_D)}^{(\omega_S)}(m,n) = \frac{(\omega_2 \mp \omega_1)}{\hbar^2} & \left\{ \frac{1}{(\pm \omega_1 - \omega_{mg} + i\Gamma_{mg})(\omega_2 - \omega_{mg} + i\Gamma_{mg})(\pm \omega_1 + \omega_2 - \omega_{mn} + i\Gamma_{mn})} \right. \\
& + \frac{1}{(\pm \omega_1 + \omega_{mg} + i\Gamma_{mg})(\omega_2 + \omega_{mg} + i\Gamma_{mg})(\pm \omega_1 + \omega_2 + \omega_{mn} + i\Gamma_{mn})} \\
& + \frac{1}{(\pm \omega_1 - \omega_{ng} + i\Gamma_{ng})(\omega_2 - \omega_{ng} + i\Gamma_{ng})(\pm \omega_1 + \omega_2 - \omega_{ng} + i\Gamma_{ng})} \\
& \left. + \frac{1}{(\pm \omega_1 + \omega_{ng} + i\Gamma_{ng})(\omega_2 + \omega_{ng} + i\Gamma_{ng})(\pm \omega_1 + \omega_2 + \omega_{ng} + i\Gamma_{ng})} \right\}. \quad (7)
\end{aligned}$$

The summation on  $m$  and  $n$  is over the complete basis set. The  $\omega_{mn}$  and the  $\mu_{mn} \equiv \langle m | \hat{\mu} | n \rangle$  are the Bohr angular frequencies and transition moments in the basis set for which the index  $g$  is reserved for the ground state.  $\Gamma_{mn}$  is the dephasing rate constant for the macroscopic coherence between states  $m$  and  $n$ . It is also the half width at half maximum (HWHM) of the (Lorentzian) spectrum of the pole in which it appears.  $\Gamma_{mn}$  is usually composed of a population-decay term and a pure-dephasing term. The former, written as  $(1/2)(\Gamma_{mm} + \Gamma_{nn})$ , is just the arithmetic mean of the reciprocal lifetimes of states  $m$  and  $n$ . The latter, denoted by  $\Gamma'_{mn}$ , is the *pure-dephasing* rate constant—that for the elastic dephasing processes. As is well known, if  $\Gamma'_{mn} = 0$  for all  $m, n$ , the bra and ket evolution becomes uncorrelated and the density-matrix approach reduces to the Rayleigh-Schrödinger perturbation treatment (within the same basis) [14].

The sum-over-states formula for second-harmonic generation (SHG) ( $2\omega = \omega + \omega$ ) may be obtained from Eq. (5) by

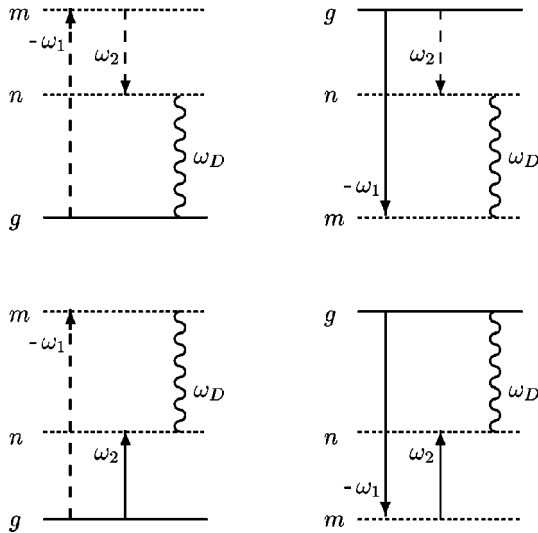


FIG. 2. The four basic WMEI diagrams for difference-frequency generation ( $\omega_D = -\omega_1 + \omega_2$ ) are shown. As in Fig. 1, solid arrows indicate *ket* evolution, dashed arrows *bra* evolution. The acting Fourier components of the two incident fields are given by their (signed) frequencies. All eight diagrams are obtained by including the permutation of the field ordering, i.e.,  $\omega_2 \leftrightarrow -\omega_1$ .

setting  $\omega_1, \omega_2 \rightarrow \omega$ , but it vanishes as is seen from the prefactor in Eq. (7). When deducing the sum-over-states expressions for the Pockels effect ( $\omega = \omega + 0$ ) and for optical rectification ( $0 = \omega - \omega$ ) from a fully dynamic sum-over-states expression, care has to be taken that both the optical frequency and their associated complex damping terms are set to zero [15,16]. It may then be shown that the Pockels effect is also symmetry forbidden in any isotropic system [15].

In deriving Eq. (5), we have assumed that the transition dipole matrix elements in Eq. (6) are real. This assumption is valid for isotropic media in the absence of an external magnetic field. From the reality condition and the antisymmetric nature of Eq. (6) it follows that  $\overline{\mu^{(3)}}(m,n) = -\overline{\mu^{(3)}}(n,m)$  and therefore, that all diagonal ( $m=n$ ) contributions to  $\overline{\beta}$  must vanish. This observation allows us to convert the double sum over intermediate states  $m$  and  $n$  into a one-sided double sum

$$\begin{aligned}
\overline{\beta}_{(\omega_D)}^{(\omega_S)} = \pm \omega_1 + \omega_2 = \sum_{m,n>m} \overline{\mu^{(3)}}(m,n) & \mathcal{F}_{(\omega_D)}^{(\omega_S)}(m,n) \\
- \mathcal{F}_{(\omega_D)}^{(\omega_S)}(n,m). \quad (8)
\end{aligned}$$

It is seen that only off-diagonal elements contribute to the sum- or difference-frequency hyperpolarizability, and that  $\overline{\beta}$  from random chiral systems has zero amplitude in the static field limit. The fragility of the isotropic component of the second-order susceptibility may be traced to this antisymmetry causing both  $\overline{\mu^{(3)}}(m,n)$  and  $\mathcal{F}_{(\omega_D)}^{(\omega_S)}(m,n)$  to be anti-Hermitian (their product, and thus, also  $\overline{\beta}$  is of course still Hermitian). This is unlike what is seen in “achiral” nonlinear susceptibilities, such as odd-order susceptibilities in isotropic media (i.e.,  $\chi^{(3)}$  giving rise to four-wave mixing processes) and even-order susceptibilities in anisotropic media (e.g., SHG, SFG, and DFG from anisotropic media such as crystals and interfaces), where diagonal contributions often dominate. It also follows that at least three states (e.g., ground state and two excited states) are required to describe second-order nonlinear processes in isotropic chiral media.

#### IV. ON MAXIMIZING $\bar{\beta}$ FOR SFG AND DFG

We now examine under what conditions  $\bar{\beta}$  (and hence,  $\chi^{(2)}$ ) become maximal. As seen in Eq. (5), there are two contributions to  $\bar{\beta}$ :  $\overline{\mu^{(3)}}$  and the energy factor  $\mathcal{F}$ . Each is considered in turn.

##### A. Optimizing $\overline{\mu^{(3)}}$

Chiral molecules possessing large transition dipoles also have the potential of offering large values for  $\overline{\mu^{(3)}}$ . However, as Eqs. (4) and (6) show, a maximal  $|\overline{\mu^{(3)}}|$  requires, in addition, that the individual Cartesian tensor components are signed such that they add constructively in the antisymmetric sum. For an examination of an electronic  $\overline{\mu^{(3)}}$ , we turn to *ab initio* calculations of  $\bar{\beta}$  for a chiral molecule possessing strong electronic transition moments, the carotenoid astaxanthin [17]. The computations confirm that for a few selected state pairs  $m, n$  the individual terms in  $\overline{\mu^{(3)}}$  are signed in a manner that is constructive and yield values of  $|\overline{\mu^{(3)}}|$  approaching the sum of the magnitudes of the individual components that make up the antisymmetric sum. The largest  $|\overline{\mu^{(3)}}|$  are of the order of  $\sim 0.3(ea_0)^3 = 0.3$  atomic units [17]. However, for small chiral molecules, the states  $m$  and  $n$  are normally located in the far ultraviolet and it would be unusual to establish specific  $m, n$  resonances without specialized experimental conditions. For small molecules, off-resonance probing that is not specific to certain excited-state pairs is thus more likely, and extensive sum-over-states calculations are necessary. We have carried this out for a few chiral molecules including the enantiomers of limonene and pinene, and are able to report an effective “many-state” value for  $\overline{\mu^{(3)}}$  that is only  $\sim 0.0012(ea_0)^3$  ( $\sim 0.02$  D<sup>3</sup>) [17]. This is much smaller than the  $\sim 0.48(ea_0)^3$  ( $\sim 8$  D<sup>3</sup>) which one might typically expect for a small molecules’ triple product of electronic transition dipoles. In the absence of resonance, the weakness of the “many-state”  $\overline{\mu^{(3)}}$  accounts for one origin of the general weakness of  $\bar{\beta}$  itself.

Next, we explore the dispersive properties of SFG and DFG through the energy factor  $\mathcal{F}$ . In particular, we show that the energy factor may, in the presence of two-state resonances, bring the strength of  $\bar{\beta}$  to a level that might be expected of a nonresonant, but dynamic, tensor element  $\beta_{ijk}$ .

##### B. Optimizing the energy factor $\mathcal{F}$ and the dispersive properties of $\bar{\beta}$

We have noted how in the static limit,  $\bar{\beta}$  must vanish as dictated by the energy factor  $\mathcal{F}$  [Eq. (7)]. And it is through this factor that resonances are possible that may dramatically enhance  $\bar{\beta}$ . In general, the first hyperpolarizability has *two* potentially resonant energy denominators. The resonant channels are best noted by referring to the WMEL diagrams in Figs. 1 and 2. In each case, it is just the upper-left diagram that offers the opportunity of a double resonance that may maximally enhance SFG and DFG, respectively.

For SFG, a one-photon resonance appears in the upper left WMEL diagram of Fig. 1 when  $\omega_1 = \omega_{mg}$  and a two-photon

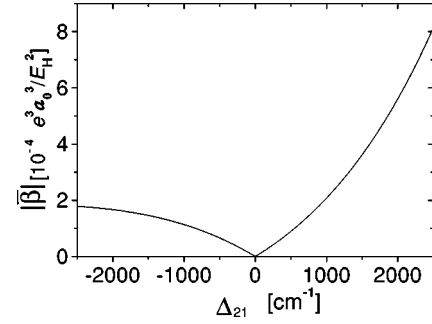


FIG. 3. The nonresonant  $\bar{\beta}$  ( $\omega_s = \omega_1 + \omega_2$ ) is shown for SFG as a function of the difference in incidence frequencies  $\Delta_{21} = \bar{\nu}_2 - \bar{\nu}_1$ . Here, the two off-resonant excited states are at 40 000 cm<sup>-1</sup> and 50 000 cm<sup>-1</sup>,  $\bar{\nu}_1$  is set at = 12 500 cm<sup>-1</sup>, while  $\bar{\nu}_2$  is tuned from 10 000 to 15 000 cm<sup>-1</sup>. All HWHM linewidths are taken to be 500 cm<sup>-1</sup>, and  $\overline{\mu^{(3)}} = 0.02$  D<sup>3</sup>.

resonance when  $\omega_1 + \omega_2 = \omega_{ng}$ . When both resonances together are operative, we see that  $\omega_2$  must be in one-photon resonance with the energy difference between the two excited states. Similarly, in the partner diagram to Fig. 1 (not shown), in which the field actions are permuted, the one-photon resonance occurs when  $\omega_2 = \omega_{mg}$  and for a double-resonance  $\omega_1$  matches the energy gap between the excited states. Whenever the two-photon resonance is present, the SFG signal itself coincides with the one-photon  $g \rightarrow n$  absorption.

Likewise for DFG, in the upper-left WMEL diagram in Fig. 2, the first step offers a one-photon resonance when  $\omega_1 = \omega_{mg}$  [or in the partner diagram (not shown) when  $\omega_2 = \omega_{mg}$ ] and then after a second step, a stimulated Raman-type two-photon resonance is possible when  $\omega_1 - \omega_2 = \omega_{ng}$ . Should both resonances be simultaneously present, then  $\omega_2$  (or  $\omega_1$  in the partner diagram) matches the energy gap between the two excited states involved in the resonances. In addition, single one-photon resonances are also available through the Feynman paths indicated by the lower-left WMEL diagrams in Figs. 1 and 2 [and their counterparts (not shown) where ordering of the field actions is permuted].

To explore these resonances, we illustrate in Figs. 3, 4, and 5 three different aspects of the influence of the energy factor  $\mathcal{F}$  on  $\bar{\beta}$ . Throughout we use the full eight-channel expression given by Eq. (7), and employ a three-state model. We also use a conservative value for the electronic effective “many-state”  $\overline{\mu^{(3)}} \sim 0.02$  D<sup>3</sup> that we obtained from *ab initio* computations of small chiral molecules. When discussing a vibrational resonance we use a  $|\overline{\mu^{(3)}}|$  that is two-orders of magnitude weaker ( $\sim 0.0002$  D<sup>3</sup>), since the triple product of transition dipoles now includes a vibrational transition moment and a Raman step. For any specific application, alternative values for  $|\overline{\mu^{(3)}}|$  may be used to scale  $|\bar{\beta}|$  appropriately.

Figure 3 presents a case where both available one-photon resonances are inactive. Here, a realistic value for a nonresonant  $|\bar{\beta}|$  for SFG is given, as the difference in incident frequencies ( $\omega_2 - \omega_1$ ) is varied. It is seen how  $|\bar{\beta}|$  increases from zero, when the incident colors are degenerate, to values

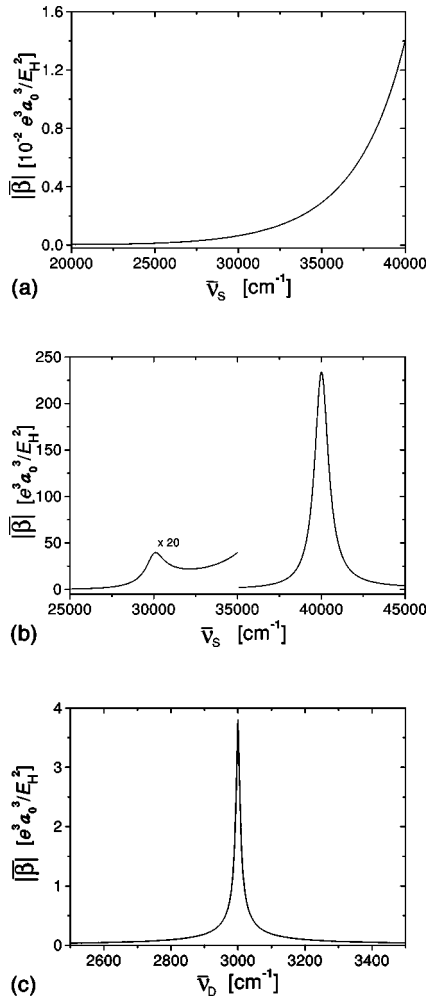


FIG. 4.  $\bar{\beta}$  in atomic units for the three-state model under various conditions of excitation. (a) Preresonant SFG ( $\bar{\nu}_S = \bar{\nu}_1 + \bar{\nu}_2$ ) is shown between 20 000 and 40 000  $\text{cm}^{-1}$ , with  $\bar{\nu}_1$  set at 8500  $\text{cm}^{-1}$ , while  $\bar{\nu}_2$  is tuned from 11 500 to 31 500  $\text{cm}^{-1}$ . The two excited states are at 50 000 and 60 000  $\text{cm}^{-1}$ ,  $\bar{\mu}^{(3)} = 0.02 \text{ D}^3$ , and the HWHM linewidths are taken to be 500  $\text{cm}^{-1}$ . (b) SFG showing two resonances as  $\bar{\nu}_S$  increases from 25 000 to 45 000  $\text{cm}^{-1}$  with the two excited states located at 30 000 and 40 000  $\text{cm}^{-1}$ .  $\bar{\nu}_2$  is tuned from 15 000 to 35 000  $\text{cm}^{-1}$  while  $\bar{\nu}_1$  is kept fixed at 10 000  $\text{cm}^{-1}$ . The HWHM linewidths are 500  $\text{cm}^{-1}$  and  $\bar{\mu}^{(3)} = 0.02 \text{ D}^3$ . A weak resonance appears when the sum frequency is two-photon resonant with the first excited state. The frequencies  $\omega_1$  and  $\omega_2$  are both off resonant. The second resonance, two orders of magnitude stronger, corresponds to fully resonant SFG. Now the sum-frequency  $\omega_S$  is two-photon resonant with the second excited state, while  $\omega_2$  is resonant with the first excited state, and  $\omega_1$  matches the energy gap between the two excited states. (c) Difference-frequency generation involving a Raman-type two-photon resonance with an infrared vibrational level. The electronic excited state is located at 40 000  $\text{cm}^{-1}$  (HWHM = 500  $\text{cm}^{-1}$ ), the vibrational state is set at 3000  $\text{cm}^{-1}$  (HWHM = 5  $\text{cm}^{-1}$ ). The difference frequency is tuned from 2500 to 3500  $\text{cm}^{-1}$  as  $\bar{\nu}_2$  changes from 17 500 to 16 500  $\text{cm}^{-1}$ , while  $\bar{\nu}_1$  is set at 20 000  $\text{cm}^{-1}$ . Here,  $\bar{\mu}^{(3)} = 0.0002 \text{ D}^3$  because of the weakened transition moments characterizing vibrational transitions.

of  $> 10^{-4} e^3 a_0^3 / E_H^2$  as the degeneracy is lifted by  $\pm 2000 \text{ cm}^{-1}$ . In this strictly off-resonant case, the choice of incident laser frequencies and excited-state energies is such that both of the potential one-photon and two-photon resonances are detuned by many bandwidths.

In Fig. 4 we examine resonance effects. First, preresonant SFG is examined in Fig. 4(a) as the sum frequency approaches from below the lowest lying of the two excited states. One of the incident frequencies is increased ( $\omega_2$ ), while  $\omega_1$  is unchanged, such that their sum moves from a detuning of 60 HWHM from the first excited state to a detuning of 20 HWHM. Over this preresonant region,  $|\bar{\beta}|$  increases by two-orders of magnitude.

In Fig. 4(b), the location of the two excited states has been lowered to permit the onset of resonances using similarly realistic laser frequencies as those in Fig 4(a). The first weak resonance appears as a two-photon resonance when the sum frequency is resonant with the first excited state. As  $\omega_2$  is increased further, a double resonance is encountered when  $\omega_2$  is resonant with the first excited state while the sum frequency becomes resonant with the second excited state. Though still based on the same conservative choice of  $|\bar{\mu}^{(3)}|$ ,  $|\bar{\beta}|$  has now reached a value of a typical nonresonant, but dynamic, electronic “achiral” tensor element  $\beta_{ijk}$ . The fully resonant  $|\bar{\beta}|$  is stronger by about six orders of magnitude compared to the off-resonant values found in Fig 3. Thus, moving from preresonance in Fig. 3 to a fully resonant situation in Fig. 4(b) would increase the SFG signal in homodyned detection by twelve orders of magnitude.

An example of DFG in the presence of a vibrational resonance is shown in Fig. 4(c). The three-level system now consists of the ground state, one excited electronic state, and one excited vibrational state. Again,  $\omega_1$  is fixed as  $\omega_2$  is tuned, but now it is their *difference* that is of concern. When this matches the vibrational state energy, the Raman-type two-photon resonance is activated. The electronic state is located such that the potential one-photon resonance is inactive. Even though the conservative choice for  $|\bar{\mu}^{(3)}|$  in this process is smaller by two orders of magnitude compared to a purely electronic triple product of transition dipoles, a remarkable resonance enhancement of  $|\bar{\beta}|$  is observed. An increase of four orders of magnitude is seen over the values found in Fig. 3. This is due to the relatively narrow linewidths (such as HWHM  $\sim 5 \text{ cm}^{-1}$ ) that characterize vibrational transitions.

## V. CHIRAL DEPHASING LINE SHAPES

We emphasize that in the electric dipole approximation, only chiral centers may contribute to coherent SFG and DFG in an isotropic medium. Consequently, a sum- or difference-frequency signal from a chiral liquid offers the unique opportunity to study background-free chiral-specific dynamics including dephasing dynamics.

To illustrate this point, we explore in Fig. 5, nonresonant SFG in a chiral three-level system in which the sum frequency is tuned such that it encompasses the energy gap between the two excited states in the model while avoiding

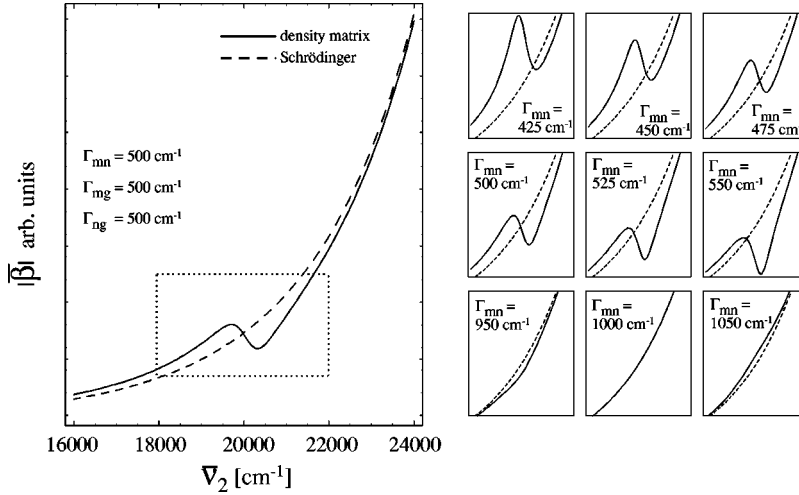


FIG. 5. Dephasing dynamics in a chiral three-state model: pure-dephasing-induced extra resonances.  $|\bar{\beta}|$  is shown for nonresonant SFG as the sum frequency varies to encompass the energy gap between the two excited states of the three-state model. Results both from the density-matrix approach—as presented in the text—(solid line) and from the Rayleigh-Schrödinger formalism (dashed line) are shown. The excited states are located at 40 000 and 70 000  $\text{cm}^{-1}$ ,  $\bar{\nu}_1$  is fixed at 10 000  $\text{cm}^{-1}$ , while  $\bar{\nu}_2$  is tuned from 16 000 to 24 000  $\text{cm}^{-1}$ . Under these conditions, neither the one-photon resonance nor the two-photon resonance available at second order can appear. Nevertheless, when  $\bar{\nu}_2 = 20\,000 \text{ cm}^{-1}$  ( $\bar{\nu}_s = 30\,000 \text{ cm}^{-1}$ ), a curious feature appears in the density-matrix treatment that is absent in the Rayleigh-Schrödinger formalism. This feature is seen to be highly sensitive to the value chosen for the damping rate constant of the  $mn$  coherence (see inset). It vanishes altogether when  $\Gamma_{mn} = 1000 \text{ cm}^{-1}$ . Since we choose  $500 \text{ cm}^{-1}$  for the HWHM of each of the poles at  $\omega_{mg}$  and  $\omega_{ng}$ , the pure-dephasing rate constant  $\Gamma'_{mn} \neq 0$  as long as  $\Gamma_{mn} \neq 1000 \text{ cm}^{-1}$  (see [14]). Thus, this special feature is a clear case of a pure-dephasing-induced extra resonance, which, in the present case of SFG from an isotropic medium, is necessarily also chiral specific.

the normal one- and two-photon resonances available to the first hyperpolarizability. This is accomplished by fixing  $\omega_1$  at  $\bar{\nu}_1 = 10\,000 \text{ cm}^{-1}$  (where  $\omega = 2\pi c\bar{\nu}$  with  $c$  in  $\text{cm/s}$ ), locating the first and second excited states at 40 000 and 70 000  $\text{cm}^{-1}$ , respectively, while tuning  $\bar{\nu}_2$  from 16 000 to 24 000  $\text{cm}^{-1}$ . The absence of any one- or two-photon resonance from the ground state is thus ensured, yet it does include the case where the sum frequency matches the energy gap between the two excited states. In fact, it is just at this point when a striking feature appears in the behavior of  $|\bar{\beta}|$  according to the density-matrix formalism. The dispersive variation in the line shape of  $|\bar{\beta}|$  proves to be sensitive to the value chosen for the dephasing rate constant  $\Gamma_{mn}$  of the coherence between states  $m$  and  $n$  (see inset panels in Fig. 5). Its special resonantlike behavior is absent when the pure dephasing component of  $\Gamma_{mn}$  vanishes, i.e., when  $\Gamma_{mn} = \Gamma_{mg} + \Gamma_{ng}$  [14]. This feature cannot be explained using the Rayleigh-Schrödinger perturbation theory when it is limited to the same basis set. Thus, we have found an example of a pure-dephasing-induced extra resonance in nonlinear spectroscopy that may only be understood using density-matrix theory. In the present case, this extra resonance must be chiral specific. It offers an intriguing experimental challenge to distinguish the two theoretical approaches, and suggests a special way to uncover chiral-specific dynamics.

Of course, chiral-specific SFG and DFG, when fully resonant in the normal fashion, should also offer the more conventional time-resolved (pump-probe) route for studying the dynamics that characterizes nonlinear spectroscopy.

## VI. CONCLUSIONS

Knowledge of the isotropic component of the molecular hyperpolarizability  $\bar{\beta}$ , together with the concentration of the sample, fully determine the second-order nonlinear optical properties of an isotropic medium. Nondegenerate sum- and difference-frequency generation are symmetry allowed and may exist only for an optically active medium.

An examination of the sum-over-states expression for  $\bar{\beta}$  reveals that all diagonal contributions in the double-sum vanish and that at least two nondegenerate excited states are required to obtain a nonvanishing  $\bar{\beta}$ . This is unlike what is seen in “achiral” nonlinear susceptibilities, such as  $\chi^{(3)}$  processes in isotropic media, or  $\chi^{(2)}$  processes in anisotropic media, where single-state resonances are ubiquitous.

A maximal second-order nonlinear optical response from an isotropic medium is expected to occur in a neat, resolved chiral liquid or a chiral amorphous solid in which one of the incident frequencies is in resonance with a one-photon transition from the ground state, while at the same time, a two-photon resonance from the ground state into another excited state takes place. The two-photon resonance may be either a two-photon absorption process (in SFG) or a two-photon stimulated Raman event (in DFG) into a lower level that is likely, though not necessarily, vibrational. Thus, fully resonant three-wave mixing processes in chiral systems will not only have one of the incident fields (but not both) partially absorbed by the  $g \rightarrow m$  transition, but also find the signal field coincident with the one-photon-allowed  $n \rightarrow g$  transition, where  $g$  is the ground state. Complications due to signal

reabsorption and fluorescence interference may arise that might be overcome by an appropriate detuning of the incident fields.

The requirement for nondegenerate frequencies, a noncollinear beam geometry [5], and resonance conditions will, together with the absence of phase matching, limit the utility of isotropic chiral systems as optical media for second-order nonlinear optics. However, this background-free nonlinear spectroscopy of isotropic chiral media with its special resonances is of considerable interest due to its biological and chemical relevance.

*Note added in proof.* We thank Professor J. M. Hicks for drawing our attention to Ref. [19], which also discusses

theoretical aspects of SFG in chiral liquids. We note that recently an electronically resonant sum frequency signal in optically active solutions of 1,1'-Bi-2-naphthol in tetrahydrofuran has been reported by Belkin *et al.* [20]. Our laboratory confirms these findings. It also demonstrates the chiral origin of the sum frequency signal by showing its quadratic dependence on enantiomeric excess [17].

#### ACKNOWLEDGMENTS

Aid through a grant from the NSF (CHE-0095056). P.F. is grateful for DAAD-NATO funding, and A.D.B. acknowledges support from the Leverhulme Trust.

- 
- [1] D. S. Chemla and J. Zyss, *Nonlinear Optical Properties of Organic Molecules and Crystals* (Academic Press, London, 1987).
- [2] J. Zyss, J.F. Nicoud, and M. Coquillay, *J. Chem. Phys.* **81**, 4160 (1984).
- [3] P. N. Prasad and D. J. Williams, *Introduction to Nonlinear Optical Effects in Molecules and Polymers* (Wiley, New York, 1991).
- [4] J.A. Giordmaine, *Phys. Rev.* **138**, A1559 (1965).
- [5] P. Fischer *et al.*, *Phys. Rev. Lett.* **85**, 4253 (2000).
- [6] B. Champagne, P. Fischer, and A.D. Buckingham, *Chem. Phys. Lett.* **331**, 83 (2000).
- [7] Q. Quinet and B. Champagne, *Int. J. Quantum Chem.* (to be published).
- [8] M.A. Belkin *et al.*, *Phys. Rev. Lett.* **85**, 4474 (2000).
- [9] J. Kirkwood, A. C. Albrecht, P. Fischer, and A. D. Buckingham, in *Physical Chemistry of Chirality*, edited by J. Hicks (Oxford University Press, Oxford) (to be published).
- [10] N. Bloembergen, *Nonlinear Optics, Advanced Book Classics* (Addison Wesley, Amsterdam, 1991).
- [11] Y. R. Shen, *The Principles of Nonlinear Optics* (Wiley, New York, 1984).
- [12] J.A. Armstrong, N. Bloembergen, J. Ducuing, and P. Pershan, *Phys. Rev.* **127**, 1918 (1962).
- [13] D. Lee and A. C. Albrecht, in *Advances in Infrared and Raman Spectroscopy*, edited by R. J. H. Clark and R. E. Hester (Wiley, New York, 1985), p. 179.
- [14] In the absence of pure dephasing, we have  $\Gamma_{mn} = (1/2)(\Gamma_{mm} + \Gamma_{nn})$ . Accordingly,  $\Gamma_{mg} = (1/2)(\Gamma_{mm} + \Gamma_{gg}) = (1/2)\Gamma_{mm}$ , where the last equality holds because  $\Gamma_{gg} = 0$  for the long-lived ground state. This permits one to replace everywhere  $\Gamma_{mn}$  by  $(\Gamma_{mg} + \Gamma_{ng})$ , the condition originally given [18] for recovery of the Rayleigh-Schrödinger perturbation theory from the density-matrix approach. While the Rayleigh-Schrödinger approach is correct, in order for it to capture pure-dephasing effects, its basis set must be extended to embrace states of the bath.
- [15] A.D. Buckingham and P. Fischer, *Phys. Rev. A* **61**, 035801 (2000).
- [16] A.D. Buckingham and P. Fischer, *Phys. Rev. A* **63**, 047802 (2001).
- [17] P. Fischer and A. C. Albrecht (unpublished).
- [18] N. Bloembergen, H. Lotem, and R.T. Lynch, *Indian J. Pure Appl. Phys.* **16**, 151 (1978).
- [19] P.K. Yang and J.Y. Huang, *J. Opt. Soc. Am. B* **15**, 1698 (1998).
- [20] M.A. Belkin, S.H. Han, X. Wei, and Y.R. Shen, *Phys. Rev. Lett.* **87**, 113001 (2001).